

Collisional transport in non-neutral plasmas*

Daniel H. E. Dubin^{†,a)}

Department of Physics, University of California at San Diego, La Jolla, California 92093

(Received 18 November 1997; accepted 15 December 1997)

Several recent experiments have measured collisional transport in non-neutral plasmas (heat conduction, test particle diffusion, and viscosity) that is from 10 to 10^4 times larger than predicted by classical theory. New guiding center theories of collisional transport have been developed that agree with the measurements. The experiments operate in the guiding center regime $r_c \ll \lambda_D$, where r_c is the cyclotron radius and λ_D is the Debye length. In this regime, classical transport theory is irrelevant because it implicitly assumes the opposite ordering, $\lambda_D \ll r_c$, although this ordering is not always satisfied in neutral plasmas. © 1998 American Institute of Physics.

[S1070-664X(98)93005-1]

I. INTRODUCTION

Recent theory and experiments on magnetized non-neutral plasmas have investigated the rate at which collisions cause transport of particles, energy, and momentum across an imposed magnetic field. This area of inquiry has a considerable pedigree, dating back to the early days of plasma physics, and these early efforts have come to be known as the classical theory of collisional transport.¹⁻⁴ It may be surprising that there is anything new that can be learned in this area; however, experiments observe collisional transport that is much larger than the classical theory predicts. Test particle diffusion is ten times larger than the classical theory,^{5,6} thermal transport is up to 20 times larger,⁷ and viscous momentum transport is up to four orders of magnitude larger than the classical predictions.^{8,9} These results are in substantial agreement with new theories of collisional transport.¹⁰⁻¹⁵ We will briefly review these new results here.

The observed transport is large compared to classical theory because the experiments are carried out in the guiding-center regime $r_c \ll \lambda_D$, where $r_c = \bar{v}/\Omega_c$ is the cyclotron radius, Ω_c is the cyclotron frequency, $\lambda_D = \sqrt{T/4\pi e^2 n}$ is the Debye length, $\bar{v} = \sqrt{T/m}$ is the thermal speed, T is the temperature; and n is the density. The classical theory, developed for neutral plasmas, implicitly assumes the opposite ordering, $r_c \gg \lambda_D$ (although not all neutral plasmas are in this regime), and therefore misses new transport mechanisms that come into play when $r_c \ll \lambda_D$.

In the classical theory of collisional transport, the basic transport step is caused by velocity scattering collisions as shown in Fig. 1. A binary collision produces the scattering of particle velocity vectors which results in a cross-field step of the guiding centers by a distance $\Delta r \sim r_c$. These collisions occur only for impact parameter ρ in the range $\rho \lesssim r_c$. However, when $r_c \ll \lambda_D$ most collisions have impact parameters in the range $r_c \ll \rho \lesssim \lambda_D$, and these collisions are neglected in the classical theory. The basic transport step for these long-range collisions is the $\mathbf{E} \times \mathbf{B}$ drift step shown in Fig. 2, which

looks quite different from the classical transport step. This collisional dynamics can be well-approximated by guiding center motion, as particles move across the magnetic field because of the $\mathbf{E} \times \mathbf{B}$ drift due to the long-range Coulomb interaction.

The recent experiments that observe this cross-field transport have been carried out on single species non-neutral plasmas confined in a Penning–Malmberg trap. The basic confinement geometry is displayed in Fig. 3. The trap consists of cylindrical electrodes immersed in a uniform magnetic field oriented along the axis of symmetry. Axial confinement is provided by application of voltages to the electrodes, creating an axial potential well. Radial confinement is provided by plasma rotation through the magnetic field. The plasma rotates around the symmetry axis of the trap, creating an inward $\mathbf{v} \times \mathbf{B}$ force that balances the outward electrostatic force caused by the un-neutralized plasma charge.

Non-neutral plasmas confined in Penning–Malmberg traps are excellent systems for the study of collisional transport. The plasmas can be confined quiescently for long periods of time, so that collisional effects can be observed without being masked by the large fluctuations inherent in most neutral laboratory plasmas. The signature of the collisional transport is a slow evolution toward a confined thermal equilibrium state¹⁶ in which temperature and rotation frequency are spatially uniform. This slow evolution is characterized by inward and outward fluxes of energy, angular momentum, and particles as the plasma relaxes toward thermal equilibrium.

II. SCALING OF TRANSPORT COEFFICIENTS

We first consider the cross-field energy flux, presumed to be of the form $\Gamma_T = -\kappa \partial T / \partial r$. The coefficient of heat conduction κ is related to the thermal diffusivity (or “thermometric conductivity”) χ by $\kappa = (5/2)n\chi$. (The factor of 5/2 is inserted because the general relation is $\kappa = c_p \chi$, where c_p is the specific heat per unit volume at constant pressure.) The thermal diffusivity can be thought of as a diffusion coefficient for energy, scaling roughly as the square of a step size Δr multiplied by the frequency ν_c of steps, where ν_c

*Paper gTua12-3 Bull. Am. Phys. Soc. 42, 1876 (1997).

[†]Invited speaker.

^{a)}Electronic mail: dhudubin@ucsd.edu

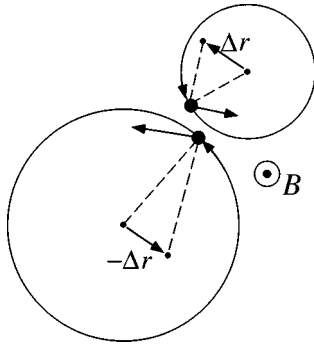


FIG. 1. Basic transport step of the classical theory. Particles (large dots) suffer a close collision, scattering their velocity vectors, and causing the guiding centers (small dots) to step across the magnetic field.

$=n\bar{v}b^2$ is a rough measure of the collision frequency (neglecting the Coulomb logarithm), and $b=e^2/T$ is the classical distance of closest approach. In the classical theory, the step size is $\Delta r \approx r_c$; that is, the energy is carried along with the particles as they step across the field, or is transferred in a collision across a distance of order r_c to another guiding center. Thus the classical thermal diffusivity is roughly

$$\chi^{\text{class}} \sim \nu_c r_c^2. \tag{1}$$

Similarly, the coefficient of shear viscosity η is related to the kinematic viscosity ν by $\nu = \eta/mn$. The kinematic viscosity is a diffusion coefficient for the momentum. Again, in classical theory momentum is transferred across the field by a distance of order r_c , leading to a classical kinematic viscosity of the same order as χ^{class} :

$$\frac{\eta^{\text{class}}}{mn} \sim \nu_c r_c^2. \tag{2}$$

In classical transport theory, both the thermal diffusivity and the kinematic viscosity scale as B^{-2} , and this leads to a conceptual difficulty. Is it reasonable that there is no transport of energy or momentum across the magnetic field in the limit of very large magnetic fields?

This difficulty is resolved by including the effect on the transport of long-range guiding center collisions such as occur in non-neutral plasmas. When the collisions are described by a Debye-shielded interaction, particles can be separated by a distance as large as λ_D and still exchange momentum and energy. The distance over which energy and angular momentum “step” in a collision time is now of order λ_D rather than r_c , so the thermal diffusivity and kinematic viscosity are independent of magnetic field, scaling as

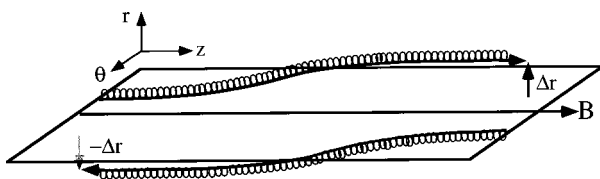


FIG. 2. Basic transport step due to long-range guiding center collisions. Particles $\mathbf{E} \times \mathbf{B}$ drift across the magnetic field due to their mutual long-range Coulomb interaction.

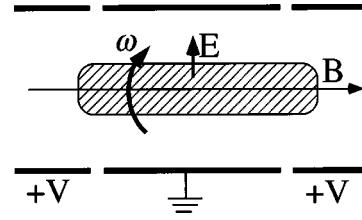


FIG. 3. Confinement geometry of a Penning–Malmberg trap.

$$\chi \sim \nu_c \lambda_D^2, \quad \frac{\eta}{nm} \sim \nu_c \lambda_D^2. \tag{3}$$

These long-range interactions allow energy and momentum to be transferred across the magnetic field even when the magnetic field is very large. It is easy to see how this happens: When guiding centers on different field lines interact, the long-range Coulomb force causes an exchange of momentum, and is responsible for the finite viscosity. Although the force transverse to the field does almost no work, since to lowest order in $1/B$ guiding centers are constrained to move along the field lines, the force parallel to the field can do work, causing a transfer of energy between the guiding centers. For example, the two guiding centers can exchange their parallel velocities in the collision.

Rigorous calculations of the thermal conductivity¹¹ and viscosity^{13,14} in the guiding center regime $r_c \ll \lambda_D$ have been performed. The results for η and κ are displayed in Table I, which also displays the classical results for comparison purposes. The results for the kinematic viscosity and thermal diffusivity due to long-range Debye-shielded collisions scale as expected from Eq. (3).

Once it is recognized that long-range interactions can cause an exchange of energy and momentum, it becomes clear that the exchange is not limited to interactions over the scale of a Debye length. Particles can also exchange energy and momentum by emission and absorption of lightly damped plasma waves. Since these waves can travel great distances, the distance that energy and momentum step in an interaction is now limited only by the cross-field dimension R of the plasma: $\Delta r \sim R$. However, the effective rate at which these wave-moderated interactions occur is small compared to the collision frequency ν_c because the energy in lightly damped plasma waves is a small fraction of the total fluctuation energy in the plasma. Nevertheless, detailed calculations^{11,14} show that for a plasma which is sufficiently large, the thermal diffusivity and viscosity are dominated by wave transport. For heat transport this requires $R \geq 10^2 \lambda_D$, and for momentum transport, $R \geq 10^3 \lambda_D$ is required for the wave transport to dominate.

This wave mechanism was originally proposed by Rosenbluth and Liu¹⁷ as a possible explanation of the anomalously large heat loss through the electron channel in tokamak plasmas. More recently, Ware¹⁸ has discussed the enhancement of the wave transport for a non-Maxwellian particle distribution. The advantage of using a non-neutral plasma for experimental studies of transport is that this wave transport can be the dominant transport process.

TABLE I. Table of transport coefficients arising from like-particle collisions, assuming that v_{\min} is determined by collisions with surrounding particles.

Impact parameter range and mechanism	D	η/mn	$\chi=2\kappa/5n$
$\rho \lesssim r_c$	$\frac{4}{3} \sqrt{\pi} \nu_c r_c^2 \ln\left(\frac{r_c}{b}\right)$	$\frac{2}{5} \sqrt{\pi} \nu_c r_c^2 \ln\left(\frac{r_c}{b}\right)$	$\frac{16}{15} \sqrt{\pi} \nu_c r_c^2 \ln\left(\frac{r_c}{b}\right)$
Classical collisions			
$\rho \gg r_c$	$6\sqrt{\pi} \nu_c r_c^2 \ln\left(\frac{\bar{v}}{(D_v \sqrt{\lambda_D} r_c)^{1/3}}\right)$	$1.8 \nu_c \lambda_D^2 \ln\left(\frac{\bar{v}}{(D_v \lambda_D)^{1/3}}\right)$	$0.48 \nu_c \lambda_D^2$
$(r_c \ll \lambda_D \text{ required})$	$\ln\left(\frac{\lambda_D}{r_c}\right)$	+	+
Long-range guiding center collisions		wave contribution	wave contribution

III. MEASUREMENTS OF HEAT TRANSPORT

Preliminary measurements of heat transport in the guiding center regime have recently been performed on a pure ion plasma consisting of Mg^+ ions.⁷ The plasma is first allowed to relax toward a state of confined thermal equilibrium in which the plasma temperature is approximately spatially uniform. A local thermal gradient is then applied to the center of the plasma column by shining a laser along the magnetic field, through the center of the plasma (see Fig. 4). The plasma edge is hot in Fig. 4 because a ‘‘rotating wall’’ field is applied in order to confine the plasma for a sufficient time to approach thermal equilibrium.¹⁹ After turning off the laser, the relaxation of the applied temperature gradient is measured using a much lower intensity laser beam that probes the Doppler-broadened width of a resonance line in the ion spectrum. Since this measurement yields $T(r, t)$, one can obtain the thermal conductivity from the differential equation for thermal diffusion,

$$\frac{\partial(3nT/2)}{\partial t} = \nabla \cdot \kappa \nabla T, \quad (4)$$

where $3nT/2$ is the kinetic energy density of the plasma. (This equation neglects the relatively small kinetic energy associated with plasma rotation, and neglects various weak heat production mechanisms, such as heating from external field errors, the rotating wall, and collisions with neutrals.) Some preliminary measurements of the thermal diffusivity as a function of temperature are shown in Fig. 5. The measurements are taken at a single density ($n \approx 10^6 \text{ cm}^{-3}$) and a field strength of $B = 4 \text{ T}$.

These measurements are compared to the theoretical diffusivity in Fig. 5. In the experiments the plasma was insufficiently large in cross-field dimension for the wave mechanism to be important, so the thermal diffusivity should be dominated by Debye-shielded interactions,¹¹ given in Table I:

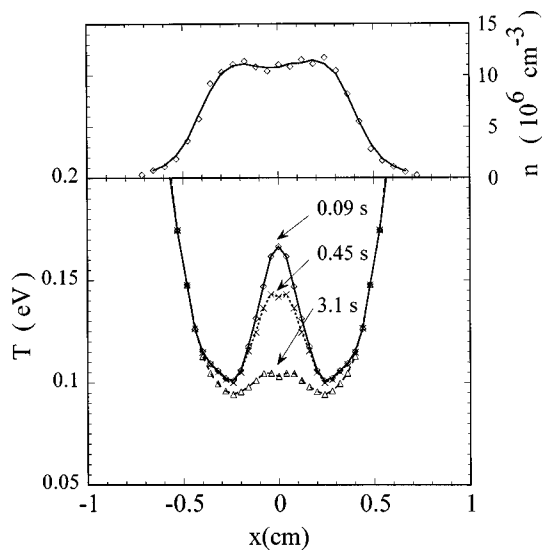


FIG. 4. Density $n(r)$ and temperature $T(r, t)$ in a pure ion plasma that has been heated locally using a laser beam oriented along the axis of the trap. The heating was turned off at time $t = 0$.

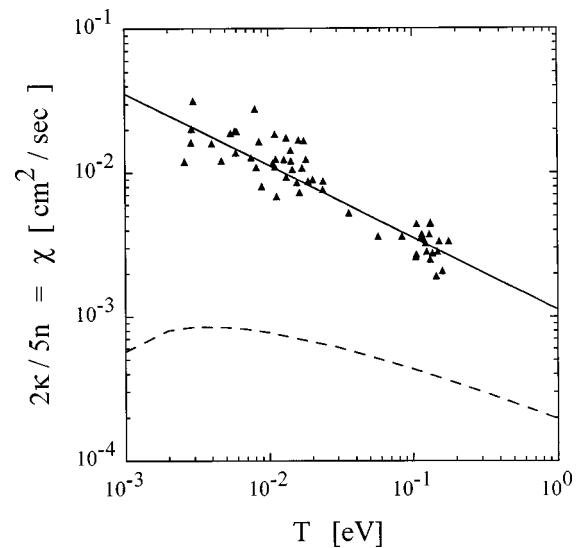


FIG. 5. Thermal diffusivity χ as a function of the plasma temperature T . Dots are preliminary experimental results, taken at a magnetic field strength of $B = 4 \text{ T}$ and at $n = 16^6 \text{ cm}^{-3}$. The dashed curve is the classical theory. The solid curve is the long-range guiding center theory prediction, given by Eq. (5). There are no adjustable parameters.

$$\chi = 0.48 \nu_c \lambda_D^2 = 0.039 \frac{e^2}{m \bar{v}}. \quad (5)$$

Equation (5) shows that χ is independent of density and magnetic field, and scales with temperature as $T^{-1/2}$. All three scalings (n, B, T) are quite different than the classical theory of Eq. (1) would predict.

The thermal diffusivity due to long-range Debye-shielded collisions [Eq. (5)] is shown as the solid line in Fig. 5. The agreement to the preliminary experimental data is quite good, with no adjustable parameters. On the other hand, the classical thermal diffusivity,⁴ shown by the dotted line for $n = 10^6 \text{ cm}^{-3}$ and $B = 4 \text{ T}$ does not match the data, and is up to 20 times too small.

IV. TWO-DIMENSIONAL BOUNCE-AVERAGED VISCOSITY

The shear viscosity of a non-neutral plasma column has also been measured in a series of recent experiments.^{8,9} However, these experiments were carried out on a different apparatus, which confined a pure electron plasma. Although the plasma was confined in the guiding center regime $\lambda_D \gg r_c$, the plasma temperature was sufficiently large that the frequency at which particles bounce along the magnetic field from one end of the plasma to the other, $\omega_b \equiv \pi \bar{v}/L$, was large compared to the fluid rotation frequency ω_r . (Here L is the length of the plasma column.) In this regime two particles on nearby field lines collide many times as they bounce back and forth along the magnetic field between the plasma ends. These correlated multiple collisions lead to an increase in the viscous transport. This effect was neglected in the scaling analysis of Eq. (3), since there particles were implicitly assumed to interact only once as they passed each other along the magnetic field.

This suggests that we consider a picture of transport due to long-range interactions between two-dimensional (2-D) charged rods (bounce-averaged electrons) which $\mathbf{E} \times \mathbf{B}$ drift due to their interactions. There has been a considerable amount of work on 2-D $\mathbf{E} \times \mathbf{B}$ drift theories of collisional transport. For example, one can show that in 2-D $\mathbf{E} \times \mathbf{B}$ drift dynamics, all dynamical times scale as the first power of B .²⁰ This implies that the cross-field particle flux driving the system toward thermal equilibrium should scale as $1/B$. This particle flux arises because shear in the rotation frequency creates an azimuthal drag force between fluid elements equal to²¹

$$F_\theta = \frac{1}{nr^2} \frac{\partial}{\partial r} r^3 \eta \frac{\partial \omega_r}{\partial r}, \quad (6)$$

where η is the local coefficient of shear viscosity. The fluid rotation frequency ω_r is given to lowest order in $1/B$ as a combination of $\mathbf{E} \times \mathbf{B}$ and diamagnetic drifts:

$$\omega_r = \frac{c}{rB} \frac{\partial \phi}{\partial r} + \frac{1}{mn\Omega_c r} \frac{\partial}{\partial r} (nT). \quad (7)$$

The theta drag force causes a $\mathbf{F} \times \mathbf{B}$ drift, yielding a radial electron flux $\Gamma_r = F_\theta cn/eB$, or

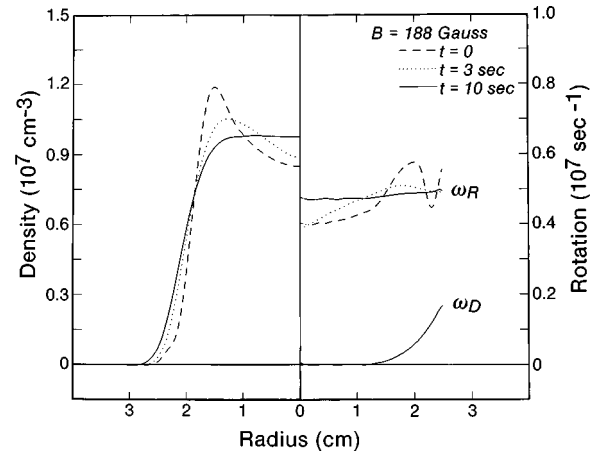


FIG. 6. Experimental plasma density profiles $n(r,t)$ and rotation profiles $\omega_r(r,t)$ at three different times t , showing the evolution to equilibrium. Here ω_D refers to the component of ω_r caused by the diamagnetic drift [see Eq. (7)]. (Taken from Ref. 8.)

$$\Gamma_r = \frac{c}{eBr^2} \frac{\partial}{\partial r} r^3 \eta \frac{\partial \omega_r}{\partial r}. \quad (8)$$

[Note that Eqs. (6)–(8) hold for both electron or ion plasmas provided that one takes e to be the signed charge, i.e., $e < 0$ for electrons.] This particle flux rearranges the density, causing the fluid rotation frequency to become uniform, as required in thermal equilibrium. Note that Γ_r will be positive at some radii and negative at others.

Since Eq. (7) implies that ω_r scales as $1/B$, and the viscous particle flux due to 2-D $\mathbf{E} \times \mathbf{B}$ collisions must scale as $1/B$, Eq. (8) implies that the viscosity due to these 2-D collisions must scale as B^1 . For sufficiently large magnetic fields [i.e., when $\omega_b > |\omega_E|$, where $\omega_E = (c/rB) \partial \phi / \partial r$ is the $\mathbf{E} \times \mathbf{B}$ rotation frequency] this 2-D viscosity is much larger than the “single collision” viscosity given by Eq. (3), which is independent of B ;¹² and of course, both of these long-range collisional viscosities are much larger than the classical velocity-scattering viscosity of Eq. (2), which scales as B^{-2} .

Evidence for B^1 scaling of the viscosity has been observed in several previous experiments on pure electron plasmas in the 2-D regime $\omega_b > |\omega_E|$. In these experiments the electron density and fluid rotation frequency were measured as a function of radius at different times. Example density and rotation profiles are shown in Fig. 6, showing evolution toward a rigid rotor rotation profile. In the early experiments⁸ the equilibration time measured from this relaxation did appear to scale as B^1 , consistent with the picture of transport due to 2-D $\mathbf{E} \times \mathbf{B}$ drifting rods.^{12,20}

More recent experiments⁹ have improved the viscosity measurement. The measured particle flux $\Gamma(r,t)$ and rotation frequency $\omega_r(r,t)$ were used to obtain the viscosity $\eta(r,t)$ via Eq. (8). Preliminary measurements of the kinematic viscosity η/nm as a function of B are displayed in Fig. 7. This data was taken at an electron density of $1.1 \times 10^7 \text{ cm}^{-3}$ and a temperature of 1 eV. The data scales roughly as B^1 , and is several orders of magnitude larger than the classical predic-

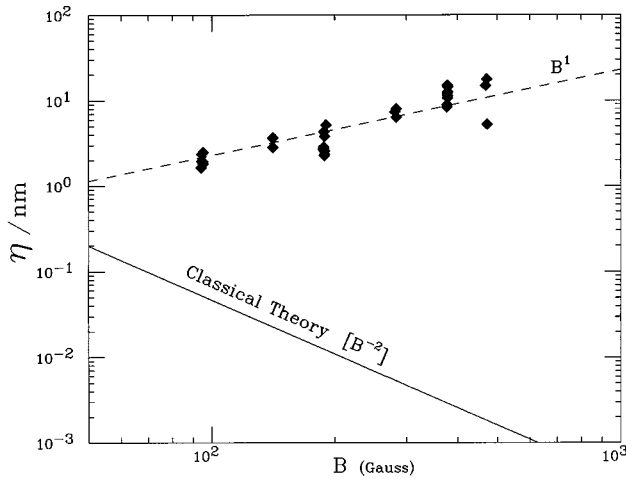


FIG. 7. Plasma kinematic viscosity η/mn as a function of applied magnetic field B . The dots are preliminary experimental measurements. The dashed line represents $\eta \propto B^1$. The solid line represents the prediction of classical theory.

tion for the viscosity,^{1,3} shown by the dotted line. The dashed line through the data merely shows B^1 scaling.

However, if one examines the 2-D $\mathbf{E} \times \mathbf{B}$ drift theory in more detail, a problem is encountered. An early 2-D $\mathbf{E} \times \mathbf{B}$ drift theory for an infinitely long plasma column¹² showed that when the $\mathbf{E} \times \mathbf{B}$ rotation frequency $\omega_E(r)$ is a monotonic function of radius, the enhanced viscous transport vanishes. However, in the experiments of Fig. 7 $\omega_E(r)$ was monotonic,⁹ and the measured flux appeared to be due to long-range interactions. Clearly, there is a problem with the theory. We believe the problem is related to the assumption that the plasma is infinitely long.

The reason that the flux vanishes in an infinite plasma column when the rotation profile is monotonic is easy to understand: resonant interactions between rods are responsible for the transport, implying that the rods must have the same $\mathbf{E} \times \mathbf{B}$ rotation frequency; that is, $\omega_E(r_1) = \omega_E(r_2)$ for rods at radii r_1 and r_2 . When $\omega_E(r)$ is monotonic, this implies $r_1 = r_2$. However, conservation of angular momentum implies that rods take equal and opposite radial steps when they $\mathbf{E} \times \mathbf{B}$ drift in their mutual Coulomb field; and if they start at the same radius there is no net radial particle flux.

However, if we allow the plasma to have a finite length, a new effect emerges: the z -averaged particle rotation frequencies now become a function of their axial speed v :²² As particles approach the ends of the plasma, they feel a confining end potential that is a function of z . The particles reverse their axial velocity, receiving a net impulse with a z component equal to $-2mv$ in this process. However, there is also a radial electric field associated with the end potential, and this radial electric field causes the particle to drift in the theta direction by an amount proportional to $2mv$. The particle's bounce-averaged $\mathbf{E} \times \mathbf{B}$ rotation frequency must therefore be written as a function of both r and v .

It is thus possible for particles at different radii to have the same rotation frequency even when the $\mathbf{E} \times \mathbf{B}$ rotation frequency is monotonic in radius, provided that the particles have different velocities. That is, the equation $\omega(r_1, v_1)$

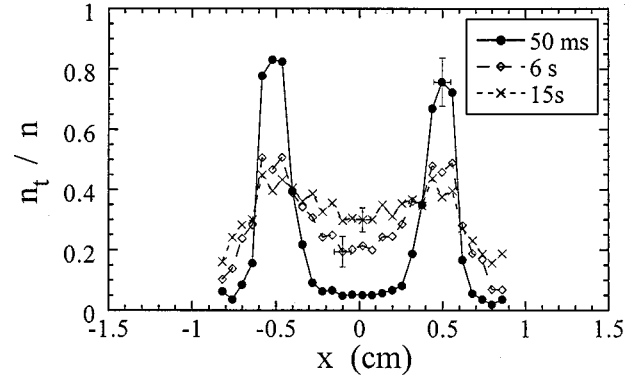


FIG. 8. Measured test particle concentration $n_t(r)/n(r)$ at three times, showing radial diffusion towards $n_t(r)/n(r) = \text{const.}$ (Taken from Ref. 6.)

$= \omega(r_2, v_2)$ can be satisfied for r_1 not equal to r_2 , provided that $v_1 \neq v_2$. A transport theory incorporating this effect is currently in preparation.¹⁵

V. TEST PARTICLE DIFFUSION

The collisional diffusion of test particles across the magnetic field has been rather thoroughly measured over a wide range of parameters.^{5,6} These experiments were carried out in the same Mg^+ pure ion plasma as the (more recent) heat transport measurements. After the plasma relaxed to near thermal equilibrium, a small population of (dynamically identical) ‘‘test’’ particles was created by placing the test particles in a different atomic spin state than the rest of the plasma using laser light. An example of the measured test particle density $n_t(r, t)$ is shown in Fig. 8. The density of test particles was observed to relax, and the test particle diffusion coefficient D was extracted by comparing the measured radial test particle flux to Fick's law,

$$\Gamma_t = -Dn \frac{\partial}{\partial r} \left(\frac{n_t}{n} \right), \quad (9)$$

which states that the flux of test particles is proportional to the concentration gradient of test particles. Note that this flux is not the same as the particle flux caused by viscous relaxation, given by Eq. (8). Test particles which are initially localized in radius will diffuse across the magnetic field even though the overall plasma is in thermal equilibrium, i.e., even though the overall density $n(r)$ does not vary in time.

The experimentally measured diffusion was then compared to the theory prediction,

$$D = D^{\mathbf{E} \times \mathbf{B}} + D^{\text{class}}, \quad (10)$$

where D^{class} is the classical theory prediction and $D^{\mathbf{E} \times \mathbf{B}}$ is the diffusion due to long-range $\mathbf{E} \times \mathbf{B}$ drift collisions. The two types of diffusion are added together because the classical result is valid for collisions with impact parameters less than r_c , while the long-range collisions due to impact parameters larger than r_c contribute to $D^{\mathbf{E} \times \mathbf{B}}$.

Furthermore, as we will now see, the classical and long-range components of D both have the same scaling with magnetic field and are roughly the same order of magnitude. (In principle, the classical viscosity and heat transport should

also be added to the long-range $\mathbf{E} \times \mathbf{B}$ contributions, but in the present experiments the classical correction is negligible for η and κ .) The scaling of the classical diffusion coefficient follows from analogous arguments to those that led to Eqs. (1) and (2): in a collision time guiding centers step a distance of order r_c due to small impact parameter velocity scattering collisions, resulting in a classical diffusion coefficient of order

$$D^{\text{class}} \sim v_c r_c^2. \quad (11)$$

The diffusion due to long-range $\mathbf{E} \times \mathbf{B}$ drift collisions can also be estimated in a similar way. Two guiding centers separated by a distance of order λ_D take a cross-field $\mathbf{E} \times \mathbf{B}$ drift step of order $\Delta t c e / (B \lambda_D^2)$, where $\Delta t \sim \lambda_D / \bar{v}$ is the time for the collision. This step is very small compared to r_c . However, the frequency of such collisions is of order $n \bar{v} \lambda_D^2$, which is large compared to the Coulomb collision frequency $\nu_c = n \bar{v} b^2$. Evaluating the resulting diffusion coefficient implies

$$D^{\mathbf{E} \times \mathbf{B}} \sim n \bar{v} \lambda_D^2 [\Delta t c e / (B \lambda_D^2)]^2 = v_c r_c^2. \quad (12)$$

Thus, the diffusion coefficient due to $\mathbf{E} \times \mathbf{B}$ collisions has roughly the same scaling as the classical coefficient. This was pointed out originally by Lifshitz and Pitaevskii.²³

A detailed calculation of the long-range diffusion coefficient^{5,10} yields

$$D_{\text{IUO}}^{\mathbf{E} \times \mathbf{B}} = 2 \sqrt{\pi} v_c r_c^2 \ln \left(\frac{\bar{v}}{v_{\min}} \right) \ln \left(\frac{\lambda_D}{r_c} \right). \quad (13)$$

The subscript IUO indicates that the technique of integration along unperturbed orbits is employed in this calculation; we will return to this point shortly. Note that the scaling of the long-range diffusion coefficient is the same as Eq. (11) for short-range collisions, as expected from Eq. (12). In fact, for the experiments, Eq. (13) predicts $D_{\text{IUO}}^{\mathbf{E} \times \mathbf{B}} \sim 3 D^{\text{class}}$. The logarithmic divergence as λ_D / r_c becomes small is due to the large $\mathbf{E} \times \mathbf{B}$ drift that arises when guiding centers undergo a close approach; the cutoff reflects the fact that the guiding center theory for the dynamics breaks down for impact parameters $\rho < r_c$. The velocity v_{\min} is the minimum relative velocity between two interacting particles for which the unperturbed orbit analysis is still valid. Particles with $v_{\min} = 0$ would interact for an infinitely long time as they move along the magnetic field, causing an infinite $\mathbf{E} \times \mathbf{B}$ drift. This is the reason for the logarithmic divergence in $D_{\text{IUO}}^{\mathbf{E} \times \mathbf{B}}$ as v_{\min} becomes small.

There are various physical mechanisms that can set v_{\min} , depending on the parameter regime of the experiments. For example, if there is shear in the mean $\mathbf{E} \times \mathbf{B}$ rotation velocity of the plasma, particles separated radially by an impact parameter ρ will move apart azimuthally with a speed $v_{\min} = \rho dv_{\mathbf{E} \times \mathbf{B}} / dr$. Collisions with surrounding particles can also determine v_{\min} since these collisions cause the relative axial velocity to diffuse. In fact these collisions are believed to be the limiting mechanism in the present experiments, giving $v_{\min} \approx (D_v \sqrt{r_c \lambda_D})^{1/3}$, where $D_v \approx v_c \bar{v}^2$ is the velocity-space diffusion coefficient, and $\sqrt{r_c \lambda_D}$ is a mean impact parameter.¹⁰

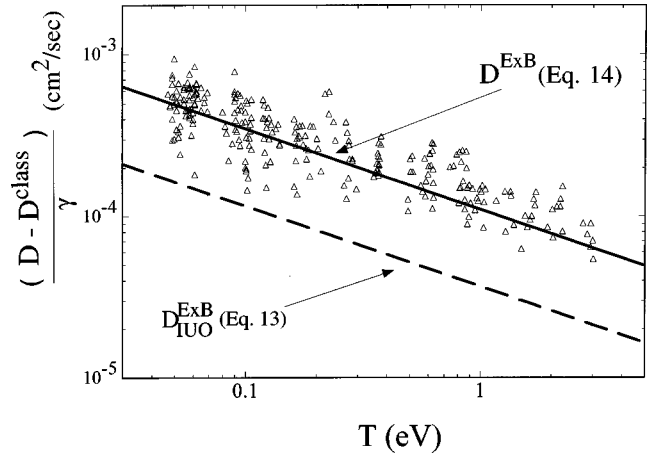


FIG. 9. The dots are the measured test particle diffusion coefficient D in cm^2/s , from which the classical result for small-impact parameter collisions, D^{class} , has been subtracted. Data are plotted versus plasma temperature T . Diffusion is normalized by the dimensionless factor $\gamma \equiv [B/1 \text{ T}]^{-2} [n/10^6 \text{ cm}^{-3}] \ln[\lambda_D/r_c] \ln[\bar{v}/(D_v \sqrt{\lambda_D r_c})^{1/3}]$ in order to display data taken at several different magnetic field strengths and densities. The dashed line is the theoretical result for long-range diffusion, $D_{\text{IUO}}^{\mathbf{E} \times \mathbf{B}}$, using IUO [Eq. (13)]; the solid line is the improved result accounting for velocity diffusion, equal to $3 D_{\text{IUO}}^{\mathbf{E} \times \mathbf{B}}$. There are no adjustable parameters. (Taken from Ref. 10.)

The long-range diffusion coefficient given by Eq. (13) is compared to the experiment in Fig. 9 (the dashed line). Here we have subtracted from the experimental measurement the classical diffusion arising from small impact parameter collisions^{1,2} given in Table I, in order to display only the diffusion due to long-range collisions [see Eq. (10)]. However, even with the classical diffusion removed from the measurement, the theory prediction for long-range collisions still falls well below the scatter of the data.

We have determined that this discrepancy is caused by a novel effect in kinetic theory.¹⁰ The diffusion coefficient in Eq. (13) was calculated using the technique of integration along unperturbed orbits (IUO). In this technique, two colliding particles are assumed to move along collisionless (unperturbed) trajectories, interacting only once as they pass by one another along the magnetic field. An uncorrelated sequence of these interactions then leads to random $\mathbf{E} \times \mathbf{B}$ steps across the field, and spatial diffusion given by Eq. (13).

However, unperturbed orbits are not a sufficiently accurate picture of the dynamics for this problem. Velocity scattering collisions with surrounding particles eventually cause the relative axial velocity of the interacting pair to reverse, and the particles have another collision; in fact, they may collide several times. This effect is neglected in IUO where particles collide only once, and it leads to a factor of 3 increase in the test particle diffusion.

One normally thinks that collisions with surrounding particles have a decorrelating effect on a given pair of particles; and in fact this is the case for particles with relative velocity less than v_{\min} , where velocity diffusion eventually causes the particles to increase their relative speed and separate. However, for particles with relative velocity greater than v_{\min} , collisions with surrounding particles have the opposite effect, ‘‘caging’’ the particles, and causing them to

interact more strongly than they would otherwise. The result of this effect is an increase in the long-range test particle diffusion coefficient by a factor of 3,

$$D^{\mathbf{E} \times \mathbf{B}} = 3D_{\text{IUC}}^{\mathbf{E} \times \mathbf{B}}. \quad (14)$$

This new prediction is shown by the solid line in Fig. 9, where it can be seen to match the experiment within the scatter of the data.

The factor of 3 enhancement depends on the fact that the collisional dynamics is effectively one dimensional, so that the velocity diffusion caused by collisions with surrounding particles reverses the relative axial velocity and leads to multiple encounters between the same pair of particles. If the particles were able to move in two or three dimensions rather than only along magnetic field lines, then a pair of particles would have an insignificant probability of having more than one encounter, and there would be no enhancement.

The factor of 3 enhancement also disappears if particles become spatially separated before they can reverse their relative parallel velocity and suffer a second collision. For example, significant shear in the background plasma can cause particles to move apart azimuthally. In the experiments to date, the plasma was nearly in a state of confined thermal equilibrium for which shears are minimal; but if the shear were made larger, one would expect the diffusion coefficient to decrease to near $D_{\text{IUC}}^{\mathbf{E} \times \mathbf{B}}$.

This factor of 3 enhancement due to multiple 1-D collisions should also be added to a previously published result¹³ for the viscosity η due to long-range collisions. This enhancement factor is included in the η of Table I. This entry also includes a factor of ~ 2 enhancement in η that arises from using the exact plasma dielectric function in the calculation rather than an *ad-hoc* Debye-shielded interaction as was used in Ref. 13. This calculation will be presented in a forthcoming paper.

VI. DISCUSSION

The new theory and experiments discussed here are leading to a new paradigm of collisional transport in the guiding center regime $r_c \ll \lambda_D$. In this regime, collisional transport is dominated by long-range guiding center collisions rather than by the close velocity-scattering collisions of classical theory. Unlike the classical theory, these guiding center collisions lead to energy transport across the magnetic field that is independent of B , allowing transport even for very large fields. The range of the transport may be further enhanced by emission and absorption of plasma waves.

In addition, correlated multiple collisions between pairs of particles are observed to strongly enhance the long-range transport. The multiple long-range collisions can be caused either by rapid bouncing of particles between the ends of the plasma (allowing a bounce-averaged 2-D analysis), or by the caging effect of velocity-scattering collisions with surrounding particles.

When the multiple collisions are caused by bouncing of the particles between the ends of the plasma, the particles can be thought of as rods of charge which $\mathbf{E} \times \mathbf{B}$ drift in their mutual interactions, leading to an enhanced viscosity that scales as B^1 . When the multiple collisions are caused by interactions with surrounding particles, the test particle diffusion and viscosity are enhanced by a factor of 3. In each case there are several issues that remain to be addressed. For example, a new row in Table I showing the bounce-averaged 2-D transport coefficients should be added.

There are several other outstanding problems for theory and experiments. For example, the effect on transport of multiple plasma species, such as several species of ions in a pure ion plasma, has not yet been studied in detail. Several transport effects not considered here will occur in such plasmas, such as centrifugal separation and thermomechanical fluxes. These problems, among others, will be addressed in several future publications.

ACKNOWLEDGMENTS

The author is indebted to Professor T. M. O'Neil, Professor C. F. Driscoll, Dr. K. S. Fine, Dr. F. Anderegg, and the rest of the UC San Diego non-neutral plasma group.

This work was supported by National Science Foundation Grant No. PHY94-21318 and Office of Naval Research Grant No. N00014-96-1-0239.

¹C. L. Longmire and M. N. Rosenbluth, *Phys. Rev.* **103**, 507 (1956).

²L. Spitzer, *Physics of Fully Ionized Gases* (Interscience, New York, 1955).

³A. Simon, *Phys. Rev.* **100**, 1557 (1956).

⁴M. N. Rosenbluth and A. N. Kaufmann, *Phys. Rev.* **109**, 1 (1958).

⁵F. Anderegg, X.-P. Huang, C. F. Driscoll, E. M. Hollmann, T. M. O'Neil, and D. H. E. Dubin, *Phys. Rev. Lett.* **78**, 2128 (1997).

⁶F. Anderegg, X.-P. Huang, E. M. Hollmann, C. F. Driscoll, T. M. O'Neil, and D. H. E. Dubin, *Phys. Plasmas* **4**, 1552 (1997).

⁷E. M. Hollmann, F. Anderegg, and C. F. Driscoll, *Bull. Am. Phys. Soc.* **42**, 1955 (1997).

⁸C. F. Driscoll, J. H. Malmberg, and K. S. Fine, *Phys. Rev. Lett.* **60**, 1290 (1988).

⁹J. M. Kriesel and C. F. Driscoll, *Bull. Am. Phys. Soc.* **42**, 1956 (1997).

¹⁰D. H. E. Dubin, *Phys. Rev. Lett.* **79**, 2678 (1997).

¹¹D. H. E. Dubin and T. M. O'Neil, *Phys. Rev. Lett.* **78**, 3868 (1997).

¹²D. H. E. Dubin and T. M. O'Neil, *Phys. Rev. Lett.* **60**, 1286 (1988).

¹³T. M. O'Neil, *Phys. Rev. Lett.* **55**, 943 (1985).

¹⁴D. H. E. Dubin and T. M. O'Neil, *Proceedings of the US-Japan Joint Institute for Fusion Theory Program* (Nagoya University, Japan, 1986), pp. 265-279.

¹⁵D. H. E. Dubin and T. M. O'Neil, *Phys. Plasmas* **5**, 1305 (1998).

¹⁶J. H. Malmberg and T. M. O'Neil, *Phys. Rev. Lett.* **39**, 1333 (1977).

¹⁷M. N. Rosenbluth and C. S. Liu, *Phys. Fluids* **19**, 815 (1976).

¹⁸A. A. Ware, *Phys. Fluids B* **5**, 2769 (1993).

¹⁹X.-P. Huang, F. Anderegg, E. M. Hollmann, and C. F. Driscoll, *Phys. Rev. Lett.* **78**, 875 (1997).

²⁰J. B. Taylor and B. McNamara, *Phys. Fluids* **14**, 1492 (1971).

²¹G. K. Batchelor, *An Introduction to Fluid Dynamics* (Cambridge University Press, Cambridge, 1967).

²²A. Peurrung and J. Fajans, *Phys. Fluids B* **5**, 4295 (1993).

²³E. M. Lifshitz and L. P. Pitaevskii, *Physical Kinetics* (Pergamon, New York, 1981), p. 273.